CHAPTER IV
RESULTS AND DISCUSSION

4.1 Characterization of Fresh Catalysts

In this project, seven catalysts were synthesized and investigated. There were two parent catalysts — Pt/HY and Pd/TiO_2; and four Pt/HY^{core}-Pd/TiO_2^{shell} catalyst with various Pd/TiO_2^{shell} composition (31 %, 36 %, 44 %, and 57 wt%) denoted as S31, S36, S44, and S57 respectively. In addition, physical mixing catalyst composed of 64 wt% Pt/HY and 36 wt% Pd/TiO_2 (denoted as S36p) was also investigated.

4.1.1 Transmission Electron Microscopy (TEM)

Transmission electron microscope (TEM) was utilized to capture images of catalysts and determine shell thickness. Figure 4.1 (a) and (b) shows TEM images of Pt/HY and the particle size is approximately 200 – 600 nm. The platinum particles (dark point) were well dispersed in the HY zeolite which could be due to the metal loading by ion-exchange method. EDX spectrum in Figure 4.1 (c) gives the peaks of Pt, Si, and Al elements which are the composition of Pt/HY catalyst. Cu, C, and O peaks observed in the EDX spectrum were from copper grid coated with a formvar film used to support the catalyst, therefore they can be ignored. Figure 4.2 (a), (b), and (c) shows TEM images of Pd/TiO_2 catalyst with 3.5 Å d spacing lattice fringes which corresponds to the spacing of (101) planes of anatase, TiO_2 (Shen *et al.* 2008). The average diameter of Pd/TiO_2 particles was 18 nm and was also observed on S31, S36, S44, and S57 catalysts. EDX spectrum in Figure 4.2 (d) gives the peaks of Ti elements which are the composition of Pd/TiO_2 catalyst. Figures 4.3 – 4.6 show TEM images of S31, S36, S44, and S57 catalysts respectively. The images exhibited that Pt/HY was fully covered with average 25 nm thickness layer of Pd/TiO_2 catalyst. However shell thickness did not increase with shell composition but instead increase the excess Pd/TiO_2 catalyst. Figure 4.3 (c) shows EDX spectrum on the outer area of S31 catalyst and observed identical spectrum as Pd/TiO_2 catalyst while EDX spectrum in the center of the S31 catalyst shown in Figure 4.3 (d) gives both Si and

Ti elements corresponded to HY and TiO_2 catalyst respectively. S36, S44, S57 catalysts also exhibited similar EDX spectra and core-shell structure can be confirmed.

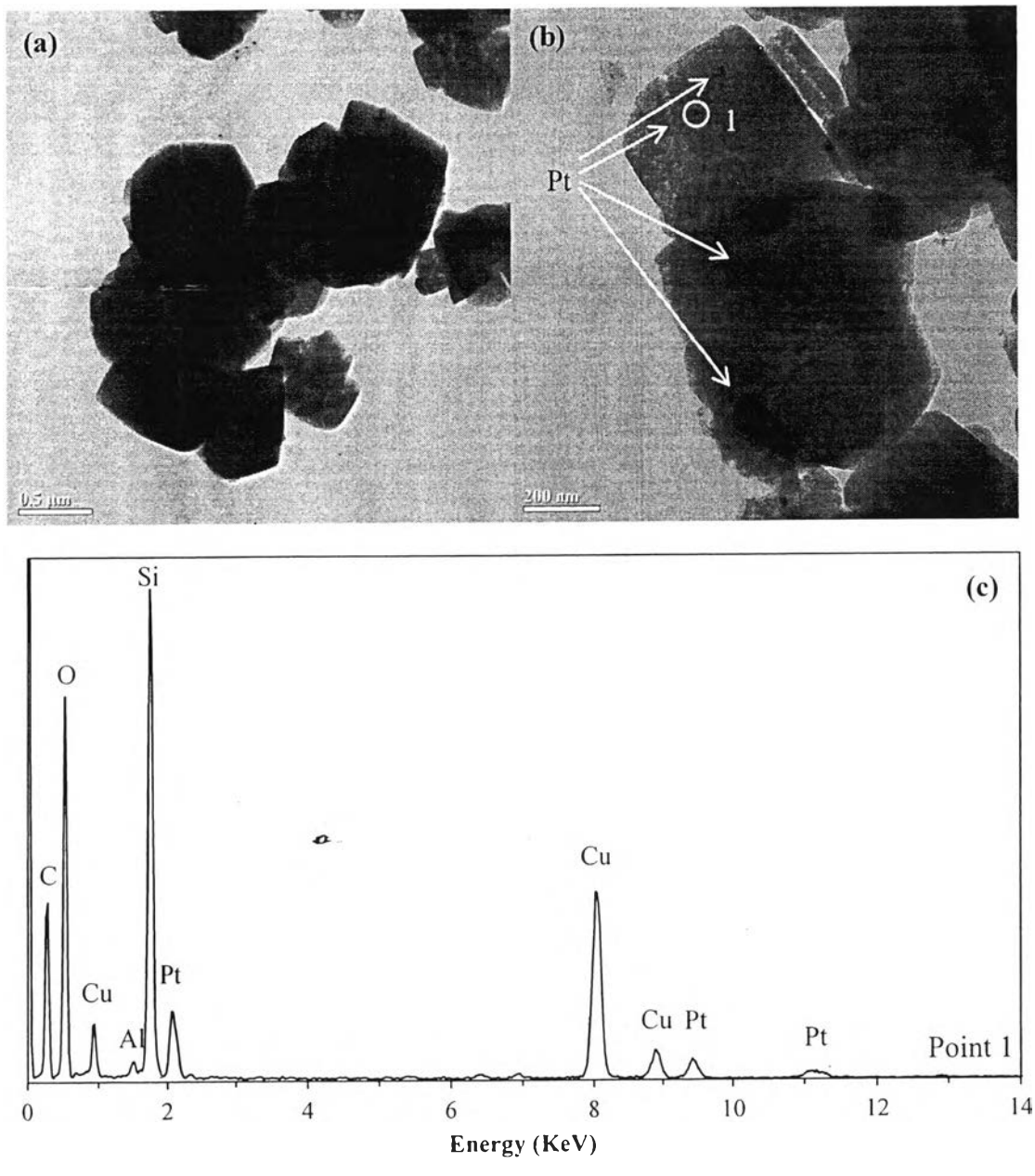

Figure 4.1 (a), (b) TEM images and (c) EDX spectrum of Pt/HY catalyst.

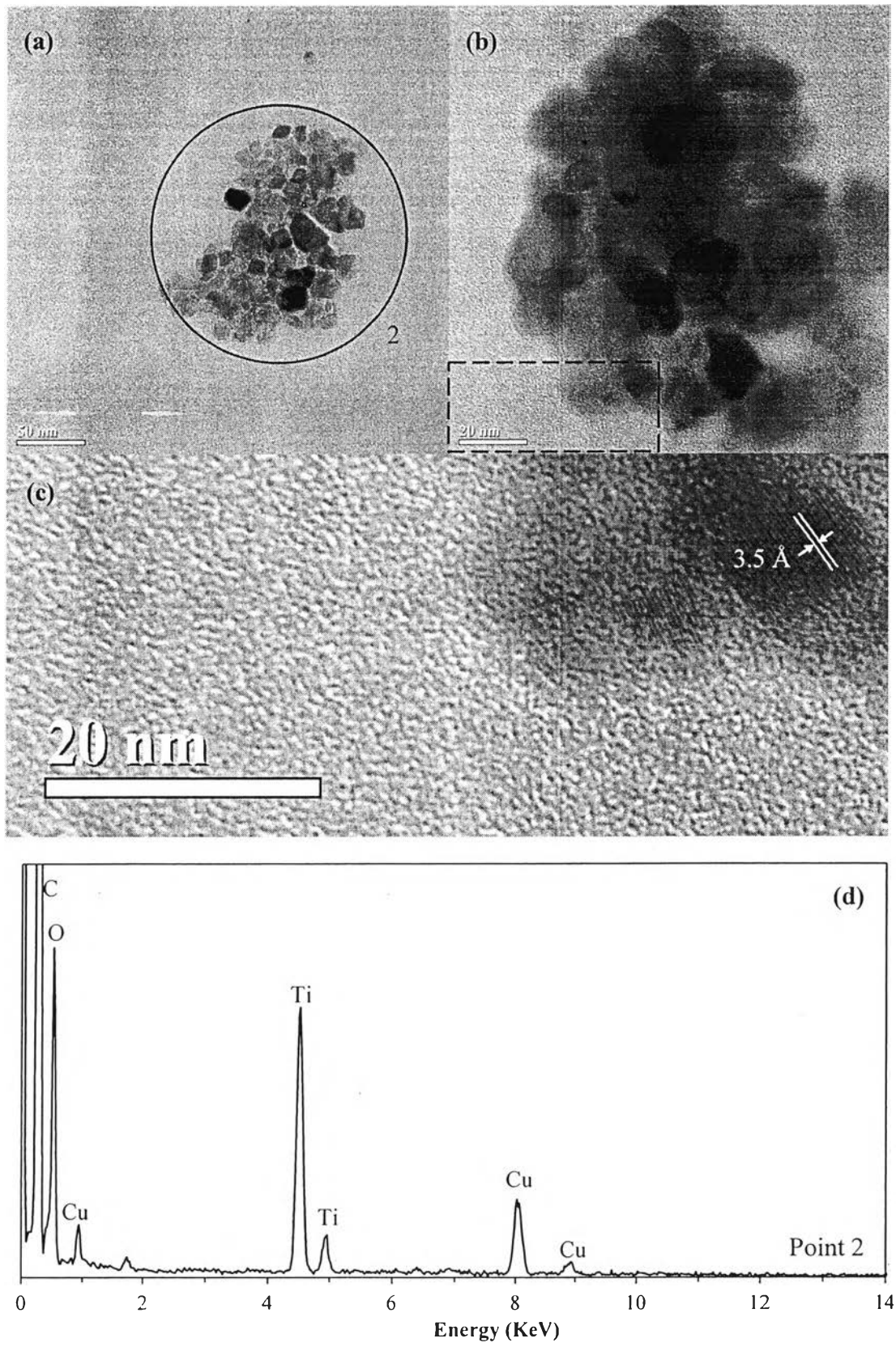

Figure 4.2 (a), (b), (c) TEM images and (d) EDX spectrum of Pd/TiO_2 catalyst.

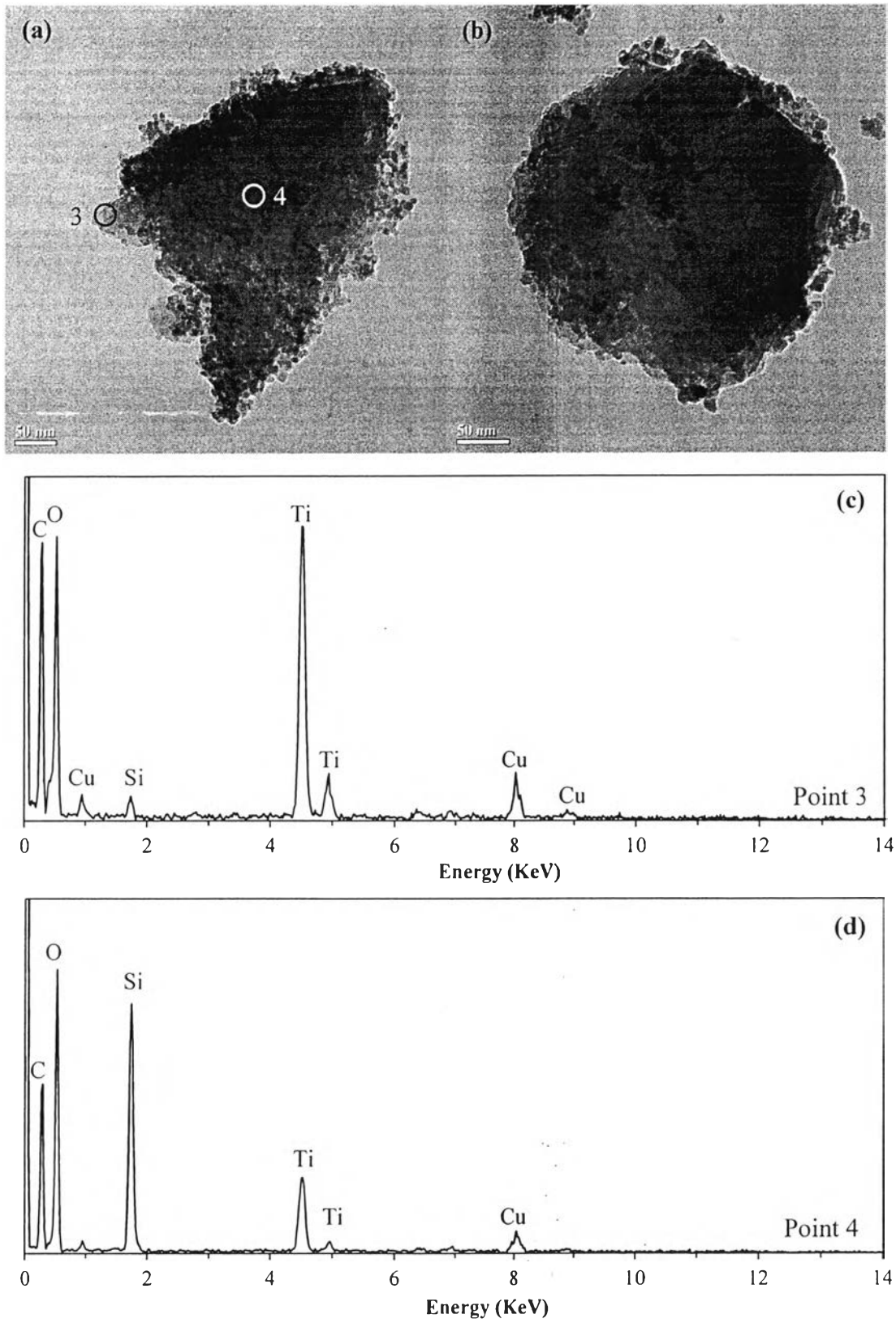

Figure 4.3 (a), (b) TEM images of S31 catalyst and (c), (d) EDX spectra of Pd/TiO_2 catalyst.

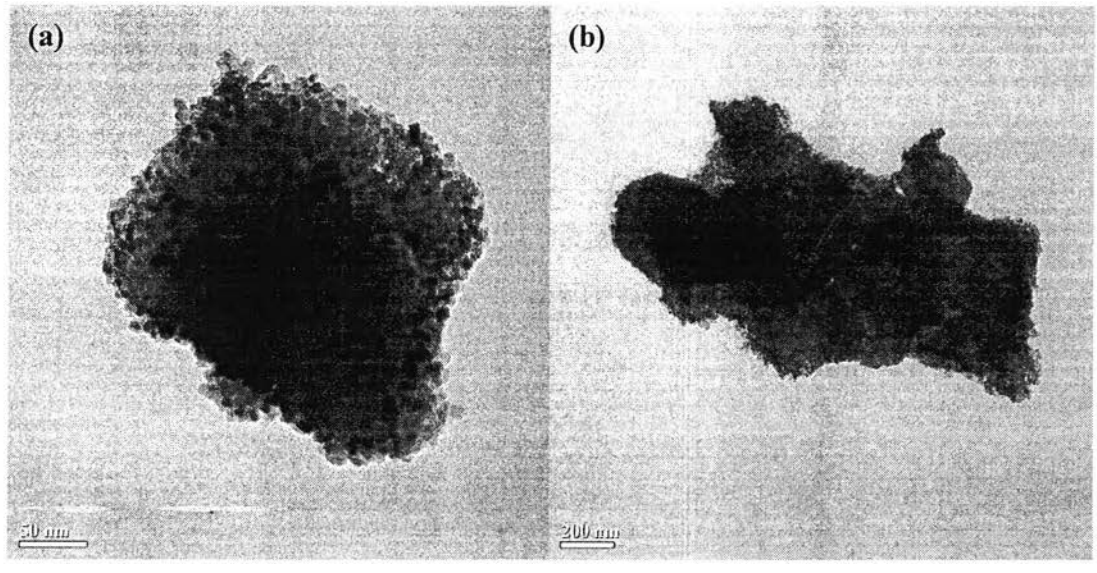

Figure 4.4 (a), (b) TEM images of S36 catalyst.

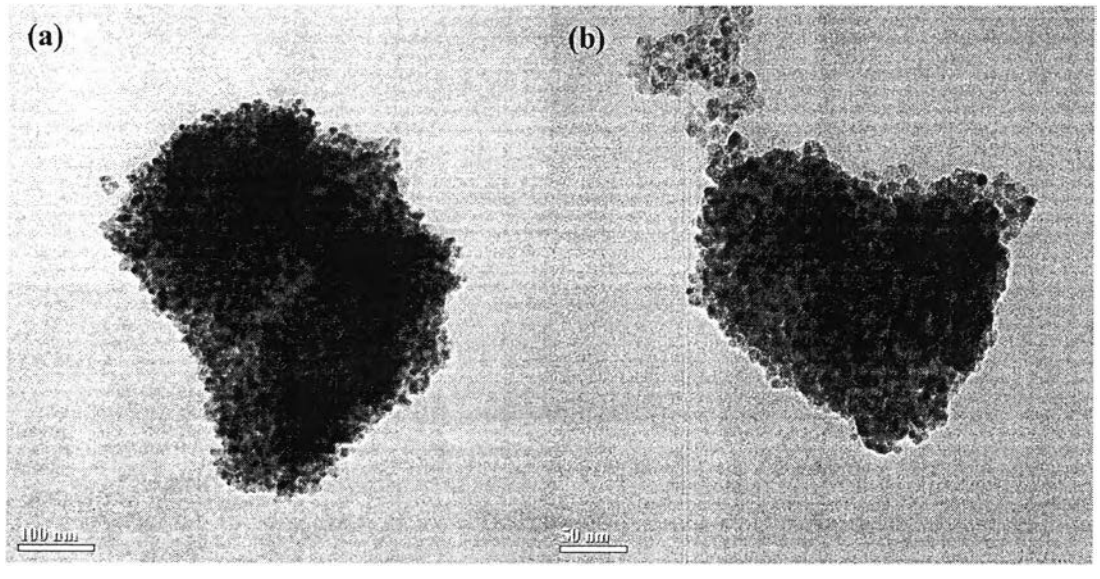

Figure 4.5 (a), (b) TEM images of S44 catalyst.

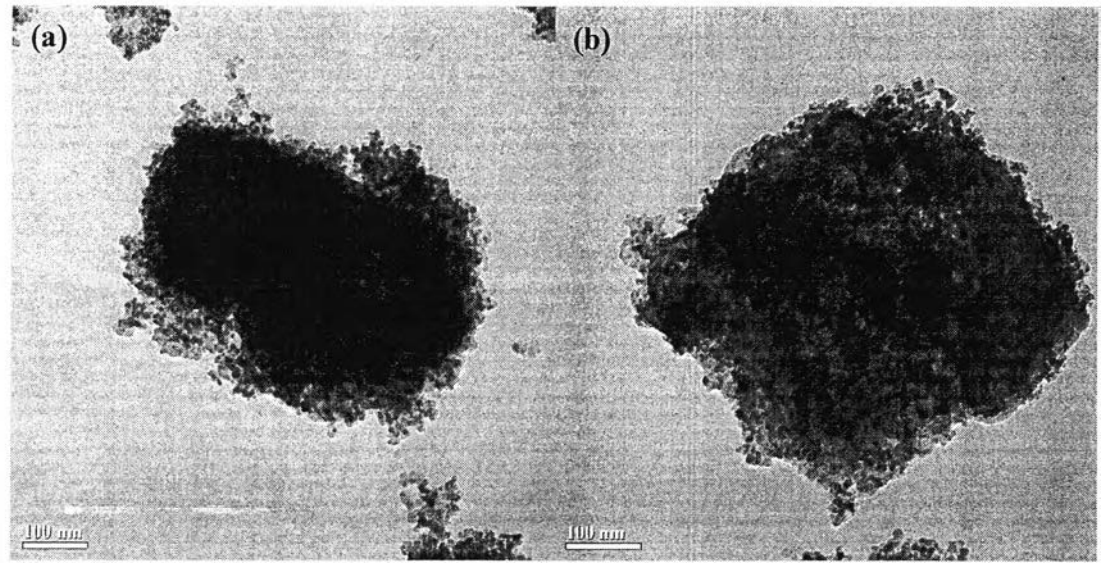

Figure 4.6 (a), (b) TEM images of S57 catalyst.

4.1.2 X-ray Diffraction (XRD)

Figure 4.7 shows XRD patterns of synthesized Pt/HY, S31, S36, S44, S57, Pd/TiO_2 catalysts. The XRD pattern of Pt/HY showed the normal diffraction pattern of HY zeolite (2θ = 6.22°, 10.19°, 11.99°, 15.83°, 18.87°, 20.57°, 21.56°, 23.08°, 23.94°, 26.11°, 27.40°, 28.09°, 30.04°, 31.17°, 31.82°, 32.91°, 33.53°, 34.56°, 35.17°, 36.15° and 38.44°). In addition, the XRD pattern of the Pd/TiO_2 catalyst indicated the crystalline structure of the pure anatase phase owing to dominant peaks at 2θ of 25.18°, 37.7°, 47.97°, 53.81°, 55.07°, 62.69°, 68.89°, 70.25° and 75° which represent the indices of 101, 104, 200, 105, 211, 204, 116, 220 and 215 planes, respectively (Yuangpho *et al.*, 2015). The XRD patterns of S31, S36, S44, and S57 catalysts showed a combined pattern of both Pt/HY and Pd/TiO_2 indicating that the prepared core-shell catalysts remained both of the parent structures.

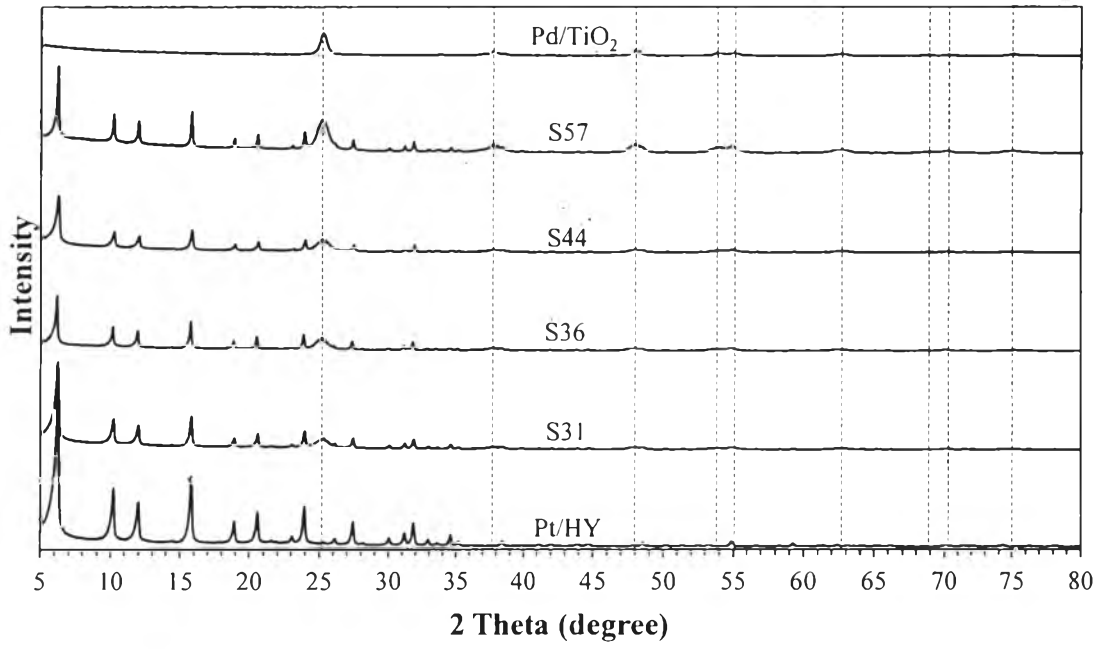

Figure 4.7 XRD patterns of synthesized Pt/HY, S31, S36, S44, S57, and Pd/TiO_2 catalysts, (dashed line: anatase).

4.1.3 Brunauer-Emmett-Tellet (BET)

The BET surface area, pore volume, and pore width were determined by N_2 adsorption-desorption analysis. From Table 4.1, the surface area, micropore and mesopore volume of Pt/HY catalyst were significantly higher than Pd/TiO_2 catalyst because microporous structure in Pt/HY catalyst and mesoporous structure in Pd/TiO_2 catalyst. The surface area and micropore volume of S31, S36, S44, and S57 catalyst decreased with Pd/TiO_2 contents, corresponding to the lower micropores in Pd/TiO_2^{shell}. Figure 4.8 shows pore size distributions of the prepared S31, S36, S44, and S57 catalysts. Pt/HY catalyst contained micropore from 6 – 14 Å and mesopore from 25 – 40 Å, on the other hand Pd/TiO_2 catalyst contained only mesopore from 34 – 82 Å. The S31, S36, S44, and S57 catalysts still remained both parent characteristics.

Table 4.1 Physical characteristics of the prepared Pt/HY, S31, S36, S44, S57, and Pd/TiO_2 catalysts.

Catalysts	BET Surface Area (m^2/g)	Pore Volume* (mL/g)	Micropore Volume* (mL/g)	Mesopore Volume* (mL/g)	Pore Width* (Å)
Pd/TiO_2	67	0.152	0.004	0.147	57.6
S57	354	0.389	0.125	0.264	6.14
S44	424	0.431	0.159	0.271	6.14
S36	466	0.463	0.181	0.282	6.14
S31	476	0.446	0.188	0.258	6.14
Pt/HY	636	0.516	0.268	0.248	6.14

*DFT method

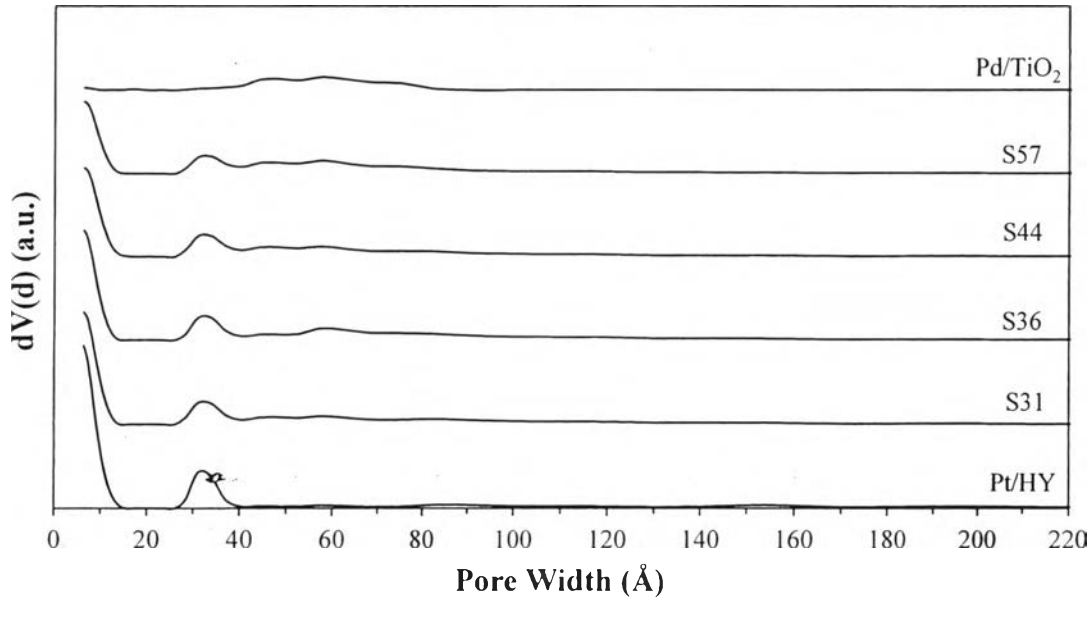

Figure 4.8 Pore size distributions of the prepared Pt/HY, S31, S36, S44, S57, and Pd/TiO_2 catalysts.

4.1.4 Atomic Absorption Spectroscopy (AAS)

Atomic absorption spectroscopy (AAS) is considered as a spectroanalytical technique for the quantitative determination of chemical elements. Therefore, this technique was employed to determine the actual metal loading of the 0.3%Pt/HY catalysts. The results revealed that the actual Pt content (wt%) on

0.3%Pt/HY was 0.2865 %. The Pt absorption signal was depressed in the presence of other noble metals and the interferences between Pt and Pd metals cannot be eliminated. Since there was no washing step in the synthesis of Pt/HY^{core}-Pd/TiO_2^{shell} catalyst, it can be assumed that all Pd, Pt contents remained in the catalysts.

4.1.5 Temperature Programmed Reduction (TPR)

Temperature programmed reduction was used to evaluate the reduction temperature of the prepared of Pt/HY and Pd/TiO_2 catalysts and the profiles are shown in Figure 4.9. The profile of Pd/TiO_2 catalyst exhibited negative H_2 consumption peak in the range of 70 – 80 °C due to the decomposition of β-PdH, which is a common feature of Pd catalysts associated with large particles. The β-PdH have been formed during the TPR experiment during the initial flushing of the catalyst with H_2/Ar mixture (Babu *et al.*, 2009). The large peak observed at 300 °C and 475 °C was due to the reduction of TiO_2. The reduction of Ti^{4+} to Ti^{3+} at relatively low reduction temperature was possible in the presence of Pd. The dissociatively chemisorbed hydrogen on palladium diffuse to TiO_2 and reduce Ti^{4+} to Ti^{3+} (Riyapan *et al.*, 2015). The reduction peak at 150 °C and 380 °C was observed on Pt/HY catalysts. This peak is attributed to the reduction of Pt^{4+} and Pt^{2+} respectively (Arias *et al.*, 2000) (Blomsma *et al.*, 1997). PtO_2 and PtO might have been formed during calcination and reduced to P^0 in TPR (Wijakkul, 2014). The minor peaks after the indicated peaks might come from good dispersion of Pt particles causing further H_2 consumption inside the pore. Therefore, in this work, the reduction temperature at 500 °C for treating catalysts before the catalytic activity testing was performed. The TPR patterns of Pt/HY^{core}-Pd/TiO_2^{shell} catalyst showed both parent catalyst patterns but the intensities depend on %Pd/TiO_2. The negative peaks at 70 – 80 °C were not observed in S31, S36, and S44 because the releases of H_2 were compensated for the H_2 consumption at 150 °C. The reduction peak of Pt^{4+} at 150 °C was shifted to lower temperature as shell composition increase could be due to Pd^0 promoted faster reduction temperature.

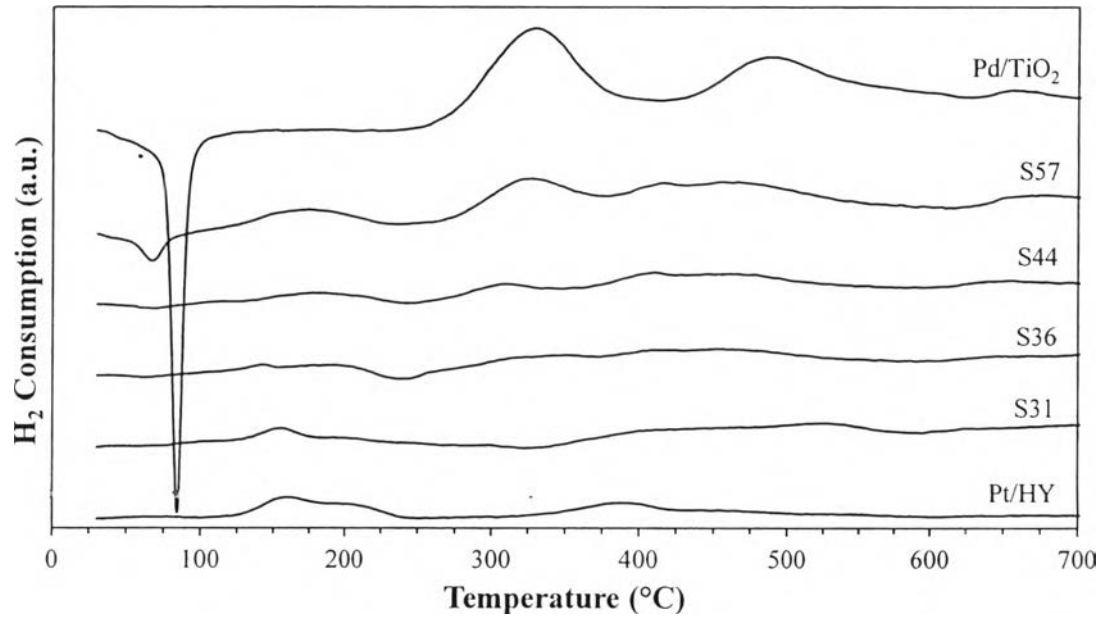

Figure 4.9 Temperature programmed reduction (TPR) profiles of the prepared Pt/HY, S31, S36, S44, S57, and Pd/TiO_2 catalysts.

4.1.6 Temperature Programmed Desorption (TPD) of Isopropylamine

Temperature programmed desorption (TPD) of isopropylamine method was used to selectively quantify Brønsted acid sites that catalyze the conversion of the isopropylamine into propylene and ammonia (Pereira and Gorte, 1992). Figure 4.10 shows TPD profiles of prepared Pt/HY, S31, S36, S44, S57, and Pd/TiO_2 catalysts. The peak at 50 – 100 °C represented physical desorption of isopropylamine. The peaks at 300 – 400 °C indicated Brønsted acid site (Kritsanakun, 2013). The acidities of prepared catalysts are summarized in Table 4.2, Pt/HY contain highest acidity and gradually decreased with Pd/TiO_2 contents.

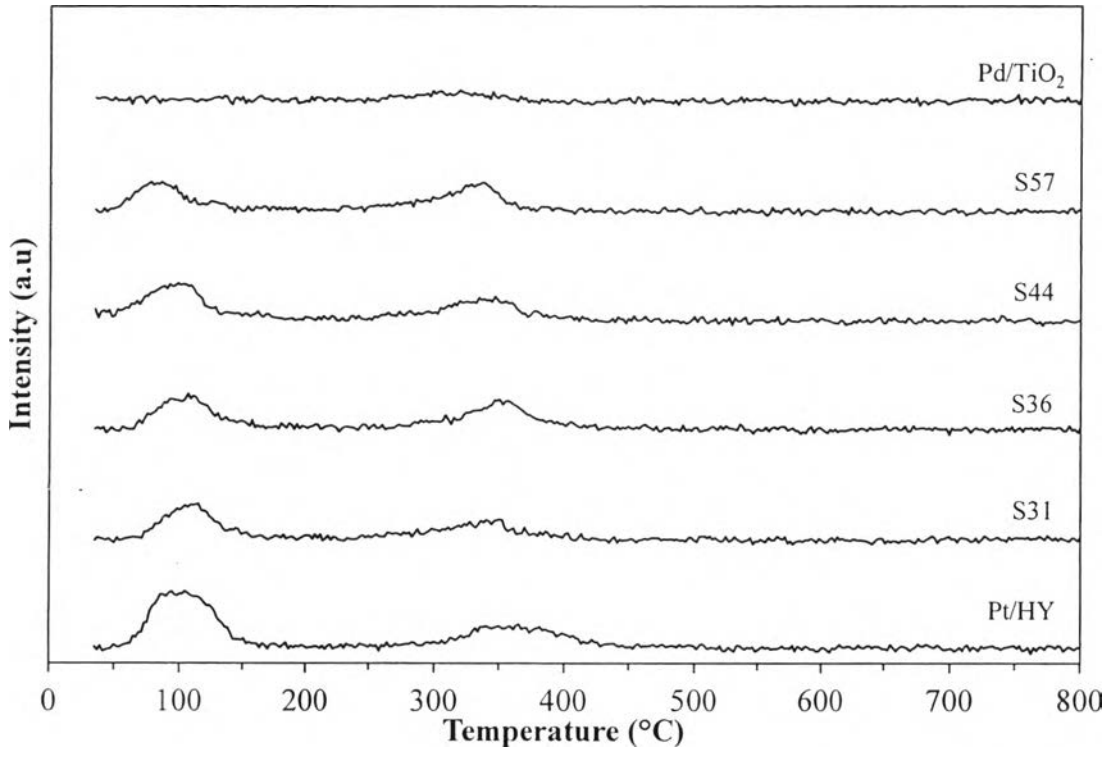

Figure 4.10 TPD profiles of prepared Pt/HY, S31, S36, S44, S57, and Pd/TiO_2 catalysts.

Table 4.2 Acidity of the prepared catalysts from TPD of isopropylamine

Catalysts	Bronsted Acidity (μmol/g)
Pd/TiO_2	5.18
S57	17.2
S44	19.2
S36	21.8
S31	22.8
Pt/HY	24.4

4.2 Standard and Feed Analyse

4.2.1 Standard Analysis

The chemical standards of products from catalytic activity testing such as hexane (n-C_6) heptane (n-C_7) octane (n-C_8) nonane (n-C_9) decane (n-C_{10}) undecane (n-C_{11}) dodecane (n-C_{12}) tetradecane (n-C_{14}) hexadecane (n-C_{16}) octadecane (n-C_{18}) were analyzed by gas chromatograph equipped with an FID detector (Agilent 7890) to identify peaks of compositions of feedstocks, intermediates and products. The chromatograms are shown in Figures 4.11. The retention time and response factor of the other standards are shown in Appendix A.

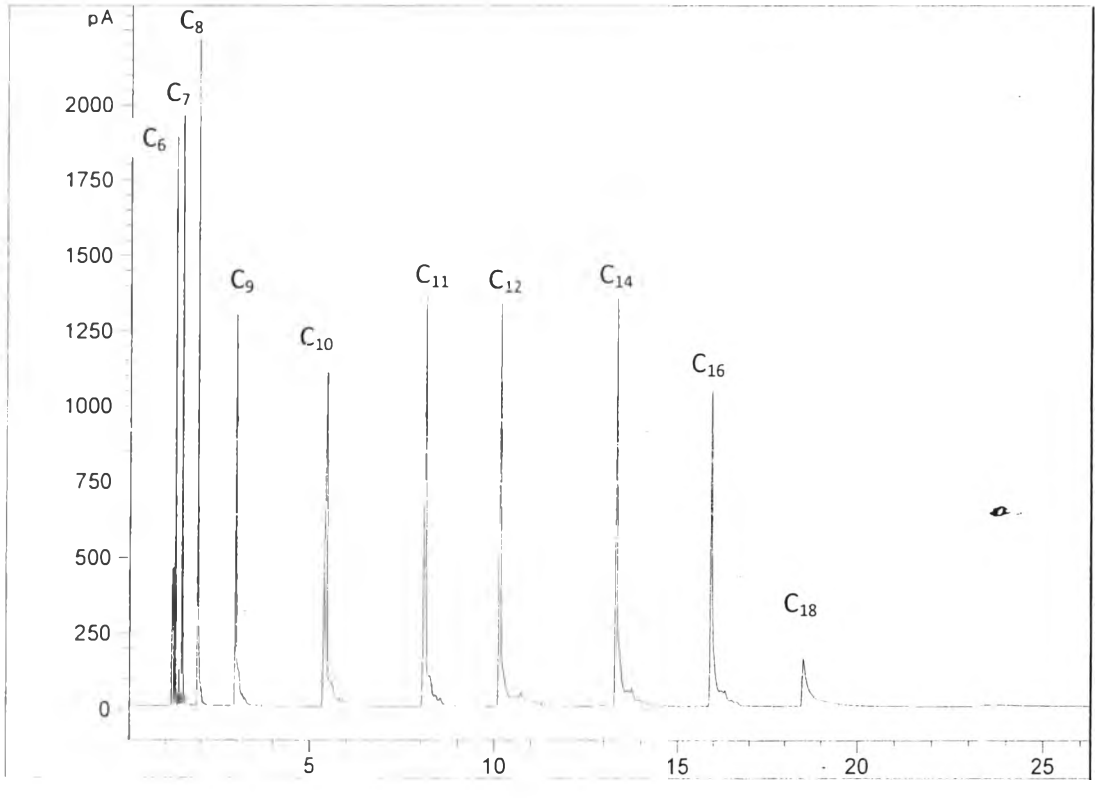

Figure 4.11 Chromatograms of standard n-alkanes.

Liquid products, chromatogram of liquid and gas products over S44 operated at operating conditions: 310 °C, 500 psig, LHSV of 0.5 h^{-1}, H_2/feed molar ratio of 60, and TOS of 4 h is shown in Figure 4.10, respectively. The liquid products on Figure 4.12 (a) are clear, colourless and less viscous on all TOS compared to

sticky yellow transparent feed jatropha oil. In Figure 4.12 (b), a chromatogram of liquid products were divided into three main parts which were gasoline fuel (C_5 – C_8), jet fuel (C_9 – C_{14}), diesel fuel (C_{15} – C_{18}) and oxygenates (palmitic acid, oleic acid, stearic acid, diglyceride, triglyceride) at the retention times of 1 – 1.9 min, 1.19 – 13.57 min, 13.57 – 20.00 min, and 20.74 – 47.00 min respectively. Finally, Figure 4.12 (c) reveals a chromatogram of gas products, consisting of light fuel (C_1 – C_4) and gasoline fuel (C_5 – C_8) at the retention times of 3.92 – 13.96 min and 15.95 – 34.13 min, respectively.

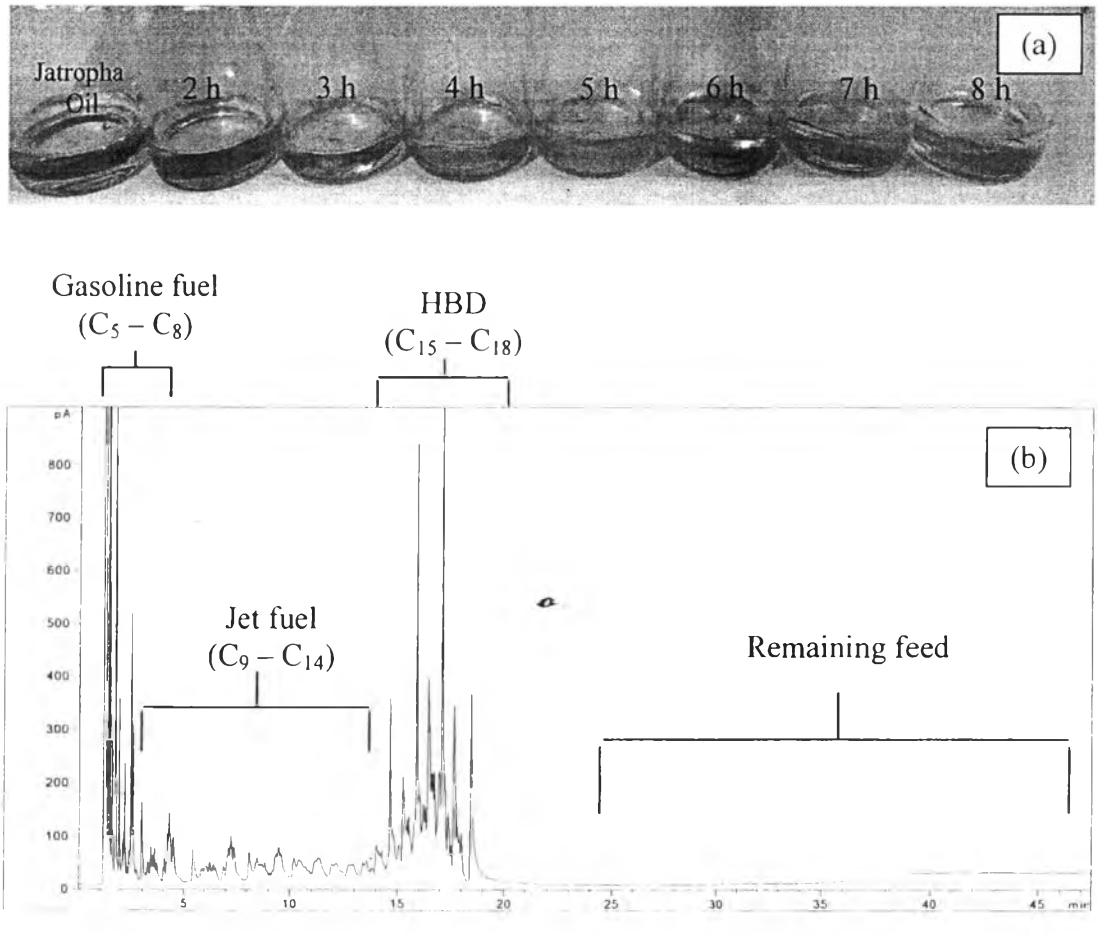

Figure 4.12 (a) Liquid products, (b) liquid products chromatogram, and (c) gas products chromatogram over S44 catalyst operated at operating conditions: 310 °C, 500 psig, LHSV of 0.5 h^{-1}, H_2/feed molar ratio of 60, and TOS of 4 h.

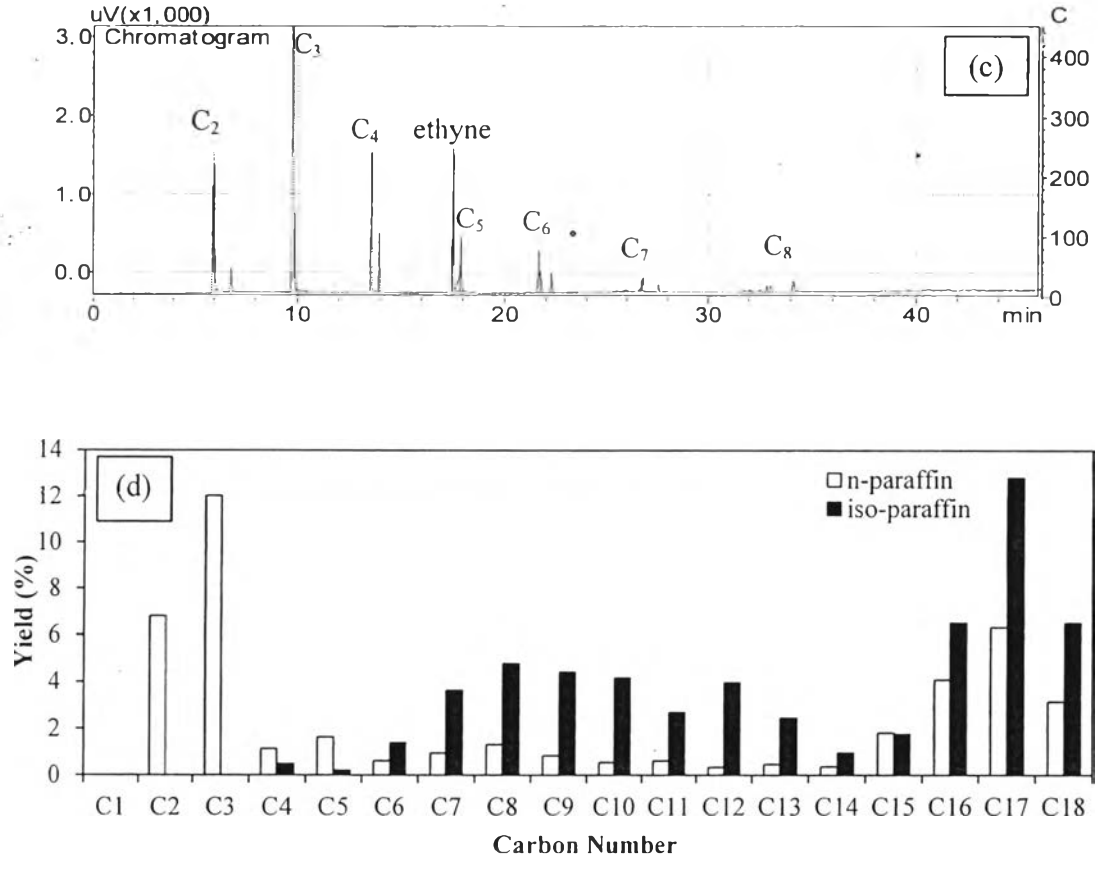

Figure 4.12 (cont.) (a) Liquid products, (b) liquid products chromatogram, (c) gas products chromatogram, and (d) Product distribution over S44 catalyst operated at operating conditions: 310 °C, 500 psig, LHSV of 0.5 h^{-1}, H_2/feed molar ratio of 60, and TOS of 4 h.

4.2.2 Feed Analysis

The jatropha oil was analyzed with gas chromatograph to identify its components. The gas chromatograph and composition of jatropha oil as shown in Figure 4.13 and Table 4.3, respectively, revealed that jatropha oil contained triglyceride as main component with trace amount of free fatty acid (e.g. oleic acid). The fatty acid composition of standard jatropha oil are listed in Table 4.4.

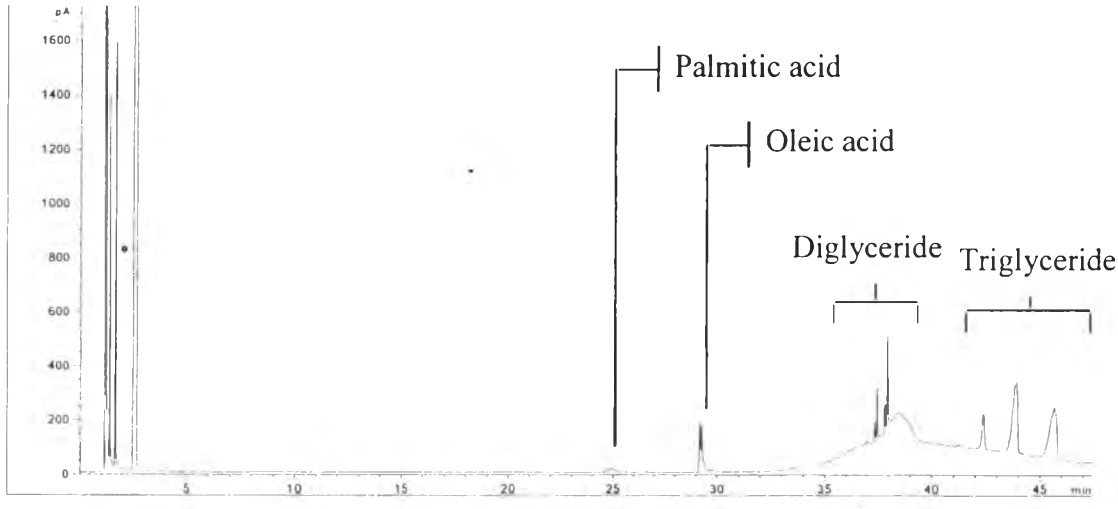

Figure 4.13 Chromatogram of jatropha oil.

Table 4.3 Composition of jatropha oil

Component	Composition (wt. %)
Triglycerides	73.21
Diglycerides	14.03
Oleic acid	11.37
Palmitic acid	1.39

Table 4.4 Fatty acid composition of jatropha oil*

Fatty Acid	Composition (wt. %)
Oleic 18:1	44.7
Linoleic 18:2	32.8
Palmitic 16:0	14.2
Stearic 18:0	7
Palmitoliec 16:1	0.7
Linolenic 18:3	0.2
Stearic 20:0	0.2
Margaric 17:0	0.1
Myristic 14:0	0.1
Caproic 6:0	0
Caprylic 8:0	0
Lauric 12:0	0
Capric 10:0	0

*From Edem, D.O. (2002)

4.3 Catalytic Activity Testing

In this section, the conversion, products yield and selectivity of one-pot reaction of jatropha oil (palmitic acid, oleic acid, stearic acid, diglyceride, triglyceride) over Pt/HY^{core}-Pd/TiO_2^{shell} catalysts with various shell compositions were investigated. The reaction conditions were 310 °C, 500 psig, liquid hourly space velocity (LHSV) of 0.5 h^{-1} and 0.9 h^{-1}, and H_2/feed molar ratio of 60.

4.3.1 Effect of LHSVs

Figure 4.14 shows the effect of LHSVs on the products yield from one-pot reaction of jatropha oil over S36 and S44 catalysts. Both catalysts and LHSVs exhibited 100 % conversion, however at LHSV of 0.9 and 0.8 h^{-1} the products are mainly diesel. When the LHSV was reduced to 0.5 h^{-1} the products were much lighter because the feed had longer time to crack and diffuse in and out of the core-shell catalyst, resulting in higher hydrocarbons with shorter chain length.

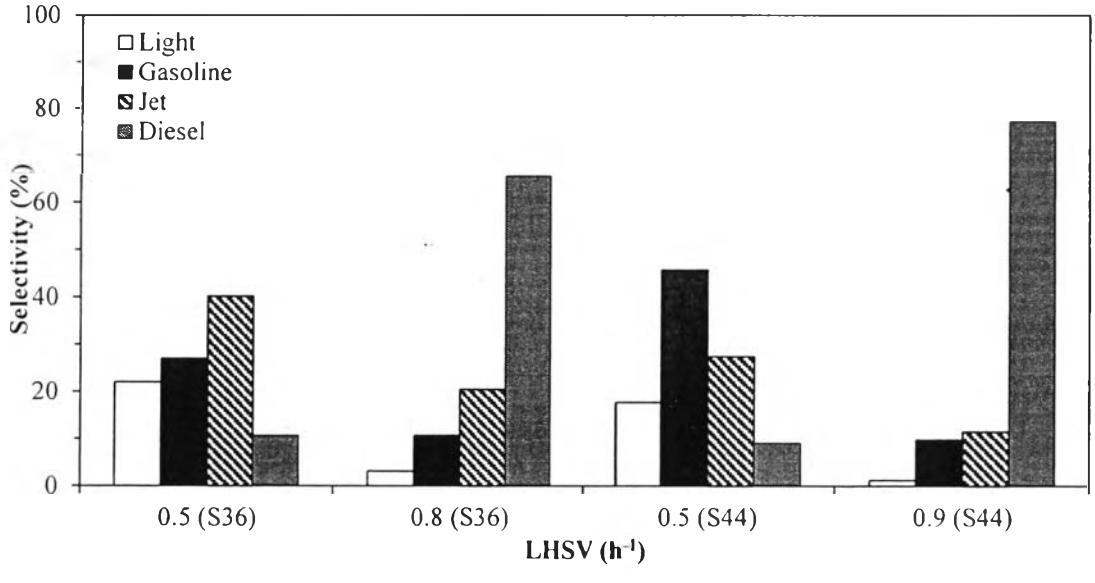

Figure 4.14 Products yield from one-pot reaction of jatropha oil over S36 and S44 catalyst at operating condition: 310 °C, 500 psig, H_2/feed molar ratio of 60, and TOS of 2 h.

4.3.2 Effect of Pd/TiO_2 Composition

Figure 4.15 and Table 4.5 show products yield from one-pot reaction of jatropha oil over Pt/HY, S31, S36, S44, S57 and Pd/TiO_2 catalysts. S31, S36, S44, and S57 catalysts exhibited 100% conversion of jatropha oil into gasoline, jet, and diesel fuel range with very high *iso*-paraffin yield due to hydrocracking and hydroisomerisation reaction which are natural function of Pt/HY. On the other hand, the conversion from Pt/HY catalyst is very low because molecule of jatropha oil is too big to enter the micro pore in Pt/HY and the products are mainly undesired fatty acids. The main product yield from Pd/TiO_2 catalyst is diesel fuel (99.6 % *n*-paraffin) with high cetane number from hydrodeoxygenation of triglycerides. S57 catalyst showed product in the longer chain range because there are less Pt/HY composition than other core-shell catalysts hence less hydrocracking and isomerisation. S36 catalyst showed the highest yield of jet fuel yield of 40.2 wt%.

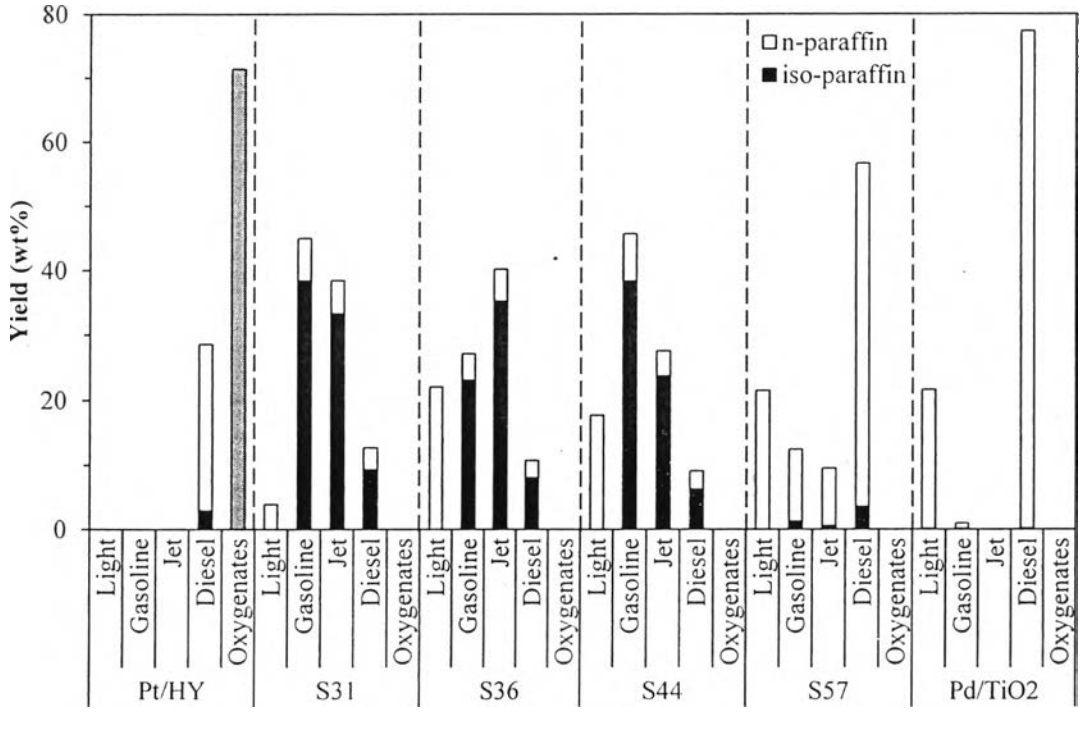

Figure 4.15 Products yield from one-pot reaction of jatropha oil over Pt/HY, S31, S36, S44, S57 and Pd/TiO_2 catalyst at operating condition: 310 °C, 500 psig, LHSV of 0.5 h^{-1}, H_2/feed molar ratio of 60, and TOS of 2 h.

Table 4.5 Liquid and gas products yield at operating condition: 310 °C, 500 psig, LHSV of 0.5 H^{-1}, H_2/feed molar ratio of 60, and TOS of 2 h.

Catalysts		Pt/HY	S31	S36	S44	S57	Pd/TiO_2
Yield of Gas Product (wt. %)	C1	0	0	0	0	0	0
	C2	0	2.13	8.10	6.64	19.69	14.09
	C3	0	1.51	12.44	9.68	1.12	7.37
	iso-C4	0	0	0	0	0	0.12
	C4	0	0.28	1.51	1.37	0.69	0.07
	iso-C5	0	0	0	0	0	0
	C5	0	0.89	0.90	2.07	8.42	0.26
	iso-C6	0	1.32	1.10	2.53	0.80	0.13
	C6	0	0.63	0.32	0.68	2.14	0.51
	iso-C7	0	2.15	0.98	1.01	0.21	0
	C7	0	0.76	0	0.25	0.19	0.03
	iso-C8	0	1.44	0	0.82	0.28	0
	C8	0	0.88	0	0.32	0.35	0.07
	iso-C9	0	0	0	0.24	0.00	0
	C9	0	0	0	0	0	0
Yield of Liquid Products (wt. %)	iso-C5	0	0.03	0	0.33	0	0
	n-C5	0	0.23	0.12	0.70	0	0
	iso-C6	0	2.12	0	0	0	0
	n-C6	0	0.27	0.17	0.41	0	0
	iso-C7	0	24.18	14.97	6.83	0	0
	n-C7	0	1.25	0.94	1.38	0	0
	iso-C8	0	7.14	6.10	26.80	0	0
	n-C8	0	1.71	1.48	1.62	0	0
	iso-C9	0	7.86	7.38	6.82	0	0
	n-C9	0	1.61	1.39	1.34	0	0
	iso-C10	0	8.35	7.68	5.73	0	0
	n-C10	0	1.12	1.10	0.89	0	0
	iso-C11	0	6.88	7.23	4.78	0	0
	n-C11	0	0.96	0.83	0.70	1.39	0
	iso-C12	0	6.12	7.15	3.84	0.58	0
	n-C12	0	0.70	0.64	0.47	7.52	0
	iso-C13	0	2.85	3.96	1.73	0	0
	n-C13	0	0.55	0.68	0.15	0	0
	iso-C14	0	1.22	1.84	0.65	0	0
	n-C14	0	0.22	0.32	0.17	0	0
	iso-C15	0.08	1.33	1.67	0.77	0.38	0
	n-C15	1.77	0.73	0.60	0.62	5.27	9.27
	iso-C16	0.33	3.67	3.53	2.75	0.36	0.03
	n-C16	1.63	1.18	0.73	0.66	4.77	3.37
	iso-C17	1.44	4.12	2.79	2.70	1.36	0.04
	n-C17	12.91	1.44	1.32	1.51	24.72	50.27
	iso-C18	1.04	0.15	0.02	0.02	1.45	0.09
	n-C18	9.40	0.03	0	0.05	18.34	14.31
Conversion		28.59	100	100	100	100	100
Yield of light (wt. %)		0	3.92	22.05	17.69	21.50	21.37
Yield of Gasoline (wt. %)		0	45.00	27.06	45.73	12.38	1.13
Yield of Jet (wt. %)		0	38.43	40.22	27.50	9.49	0
Yield of Diesel (wt. %)		28.59	12.65	10.67	9.08	56.64	77.50
Yield of Oxygenates (wt.%)		71.41	0	0	0	0	0
Sum of iso-parafins (wt.%)		2.89	80.92	69.87	68.34	5.40	0.40
Sum of n-paraffins (wt. %)		25.70	19.08	30.13	31.66	94.60	99.60

Figure 4.16 shows liquid gasoline yield over time on stream and it decreased sharply over 3 h to 4 h. Figure 4.17 shows liquid jet yield over time on stream it decrease slowly and steadily over time. Figure 4.18 shows liquid diesel yields and it increased with TOS, indicated that there are less hydrocracking. The water formed during hydrodeoxygenation may block the transportation of long chain hydrocarbon from enter the Pt/HY^{core} and resulted in mainly diesel product at late time on stream.

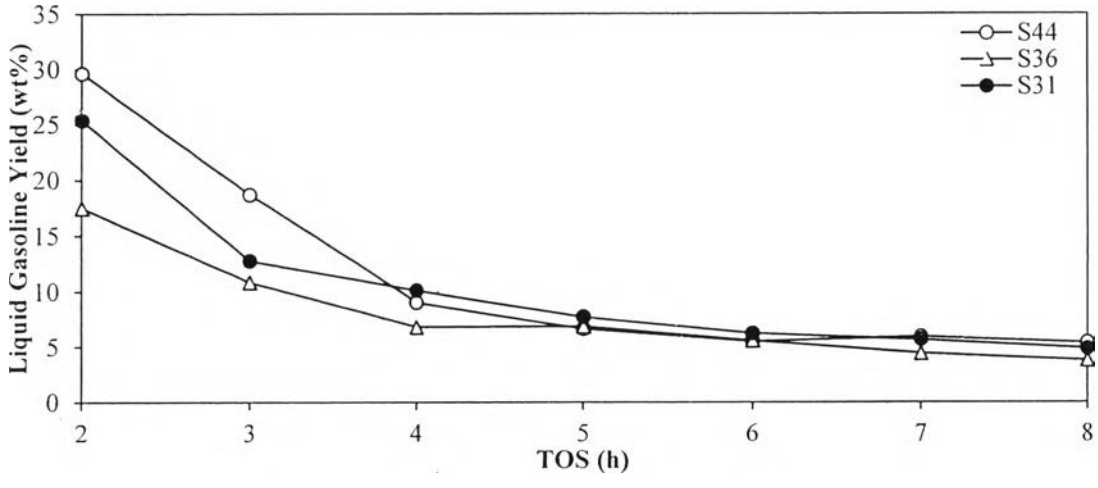

Figure 4.16 Liquid gasoline yield from one-pot reaction of jatropha oil over Pt/HY^{core}-Pd/TiO_2^{shell} catalyst at operating condition: 310 °C, 500 psig, LHSV of 0.5 h^{-1}, H_2/feed molar ratio of 60.

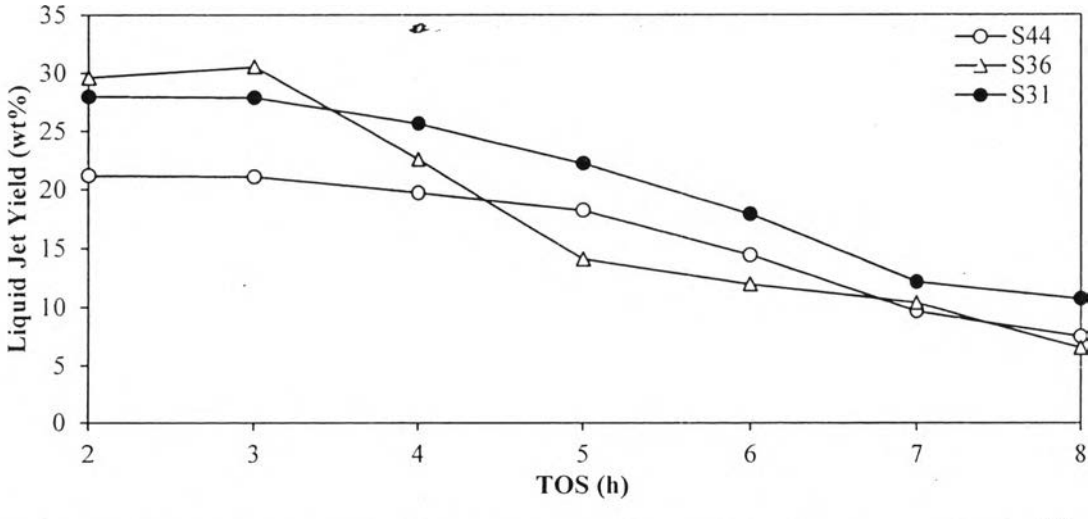

Figure 4.17 Liquid jet yield from one-pot reaction of jatropha oil over Pt/HY^{core}-Pd/TiO_2^{shell} catalyst at operating condition: 310 °C, 500 psig, LHSV of 0.5 h^{-1}, H_2/feed molar ratio of 60.

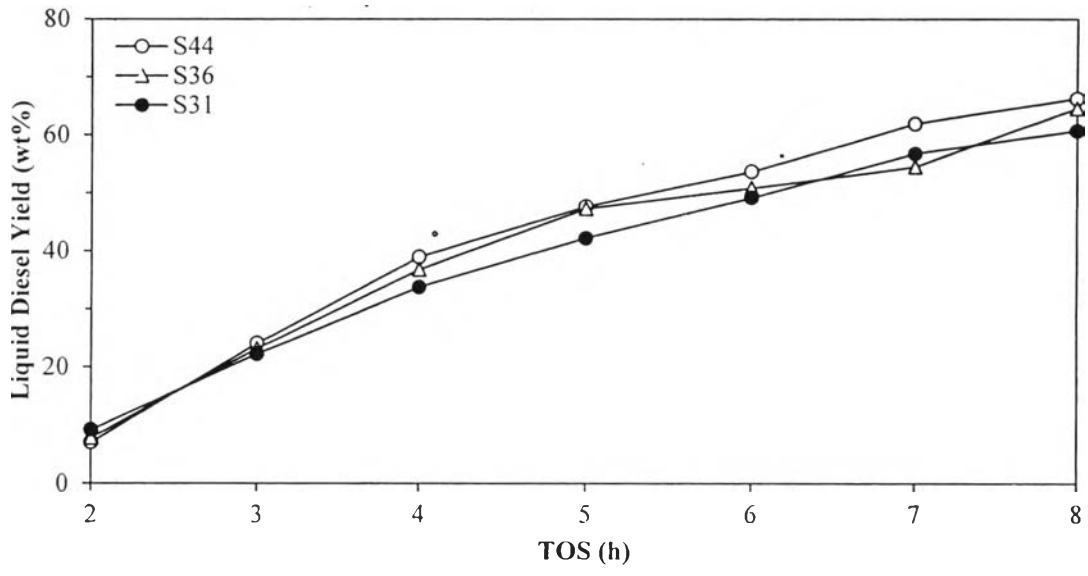

Figure 4.18 Liquid diesel yield from one-pot reaction of jatropha oil over Pt/HY^{core}-Pd/TiO_2^{shell} catalyst at operating condition: 310 °C, 500 psig, LHSV of 0.5 h^{-1}, H_2/feed molar ratio of 60.

4.3.3 Effect of Core-shell Catalysts

Figure 4.19 shows liquid products yield from one-pot reaction of jatropha oil over Pt/HY, S36, S36p, and Pd/TiO_2 catalysts. The result revealed that products over S36 catalyst were lighter than those observed over S36p catalyst. In addition, oxygenates formed rapidly as a function of time over S36p catalyst possibly because jatropha oil blocked the pore of Pt/HY compared to core-shell that Pd/TiO_2 fully covered the Pt/HY thus jatropha oil always contact with Pd/TiO_2 and deoxygenated first.

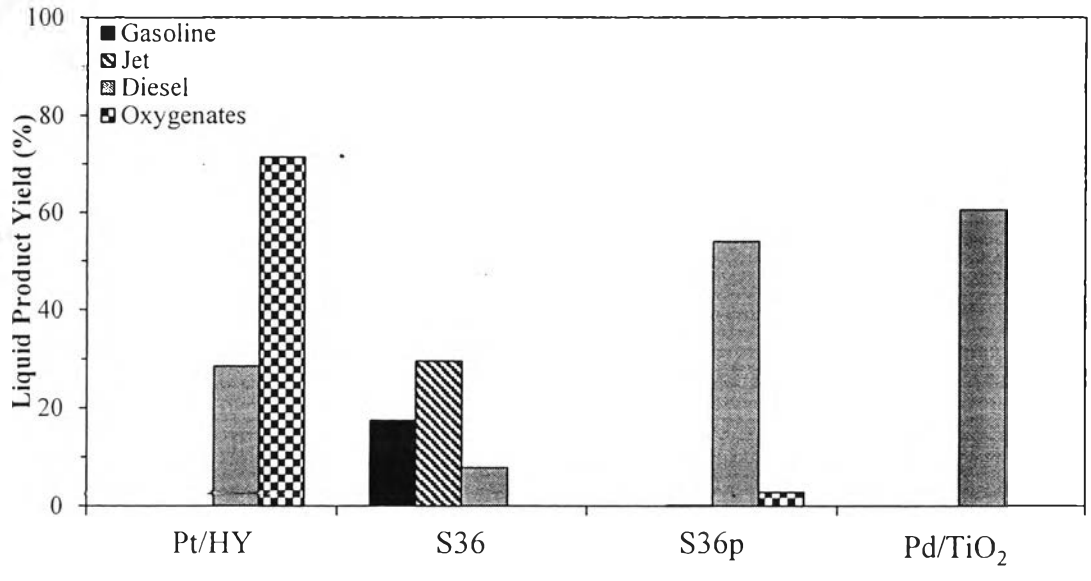

Figure 4.19 Liquid products yield from one-pot reaction of jatropha oil over Pt/HY, S36, S36p, and Pd/TiO_2 catalysts at operating condition: 310 °C, 500 psig, LHSV of 0.5 h^{-1}, H_2/feed molar ratio of 60, and TOS of 2 h.

4.3.4 Effect of Feeds

In order to evaluate the deactivation of the Pt/HY^{core}-$Pd/TiO_2{}^{shell}$ catalysts, hydrogenated biodiesel was used instead of jatropha oil and the catalytic activity result is shown in Figure 4.20. When the feed was hydrogenated biodiesel (C_{15} – C_{18}), the light, gasoline, jet fuel products are constant for 8 h of reaction comparing to jatropha oil that the short chain hydrocarbons products decrease quickly with time on stream. The jatropha oil could have poisoned Pt/HY^{core}-$Pd/TiO_2{}^{shell}$ catalyst causing the Pt/HY^{core} to deactivate.

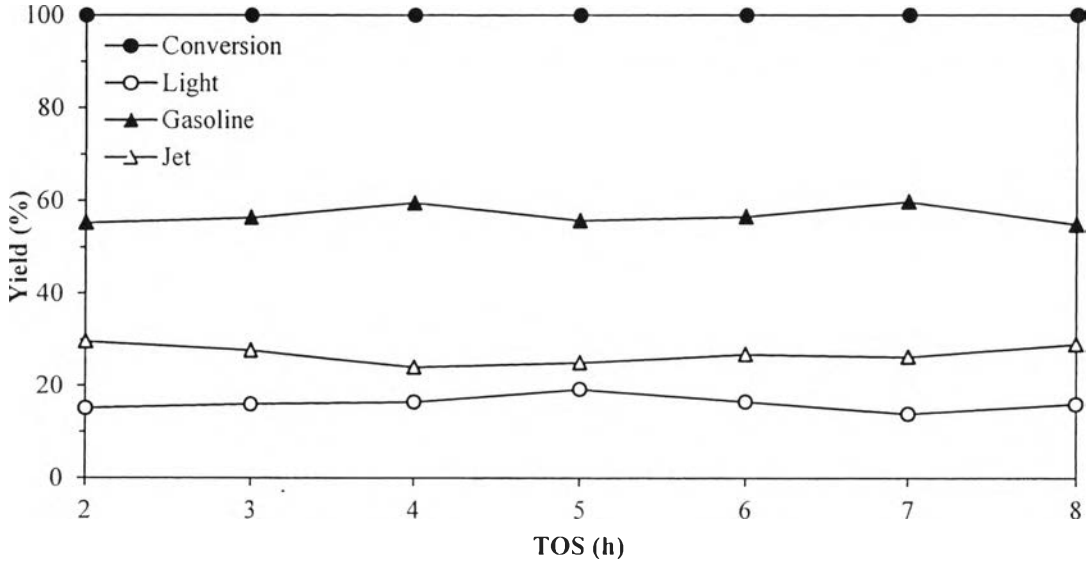

Figure 4.20 Product yields from one-pot reaction of hydrogenated biodiesel over S36 catalyst at operating condition: 310 °C, 500 psig, LHSV of 0.5 h^{-1}, H_2/feed molar ratio of 60.

4.4 Characterization of Spent Catalysts

4.4.1 Temperature-Programmed Oxidation (TPO)

The TPO profiles and amounts of coke deposit of spent catalysts after 8 h on stream are illustrated in Figure 4.21 and Table 4.6, respectively. For all catalysts, the peaks observed at temperatures below 400 °C represented the weakly coke deposit on the support. The S36p catalyst showed combined patterns of Pt/HY and Pd/TiO_2 catalysts and comparable amount of coke as S36 catalyst. S31, S36, and S44 catalysts contained higher coke than parent catalysts could be due to higher conversion of jatropha oil into lighter products.

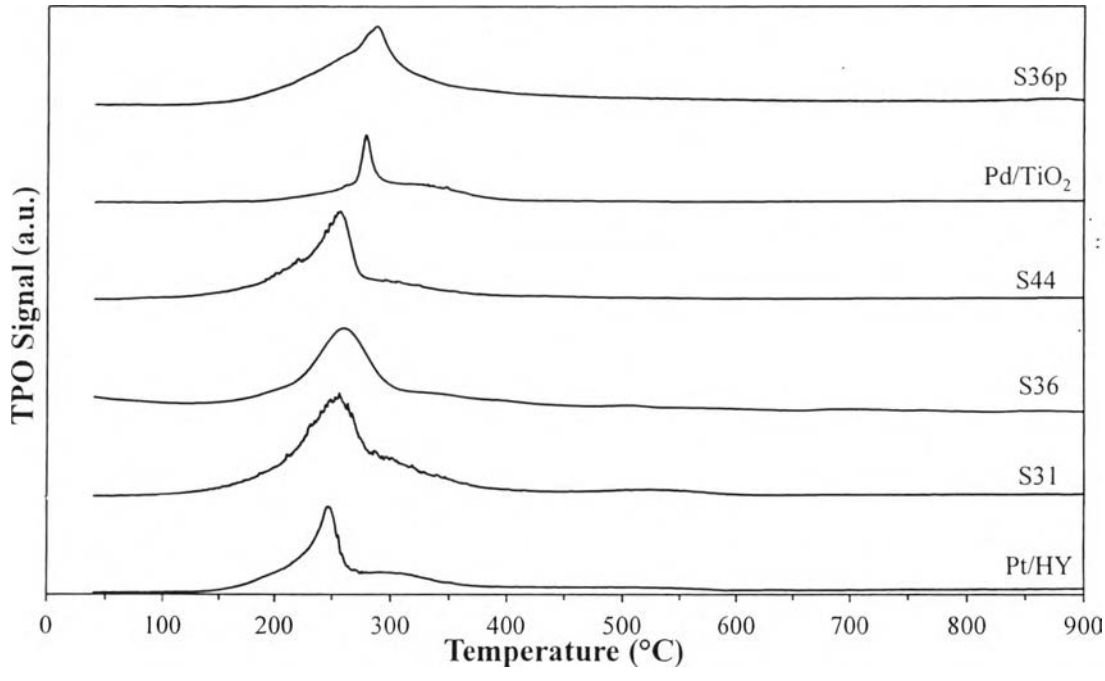

Figure 4.21 TPO profiles of physical mixing, Pt/HY, S31, S36, S44, and Pd/TiO_2 catalysts after 8 h course of reaction.

Table 4.6 Amount of carbon deposits on prepared catalyst after reaction

Catalysts	Coke (wt. %)
S36p	6.87
Pd/TiO_2	2.35
S44	5.71
S36	6.58
S31	7.26
Pt/HY	4.77

4.4.2 X-ray Diffraction of Spent Catalyst (XRD)

Figure 4.22 shows XRD patterns of Pt/HY, S36, spent S36 (after 8 h course of reaction) and Pd/TiO_2 catalysts. The XRD pattern of fresh S36 catalyst were completely the same as spent S36 catalysts indicated that 8 h course of reaction were not damaging the Pt/HY^{core}-$Pd/TiO_2{}^{shell}$ catalyst structure.

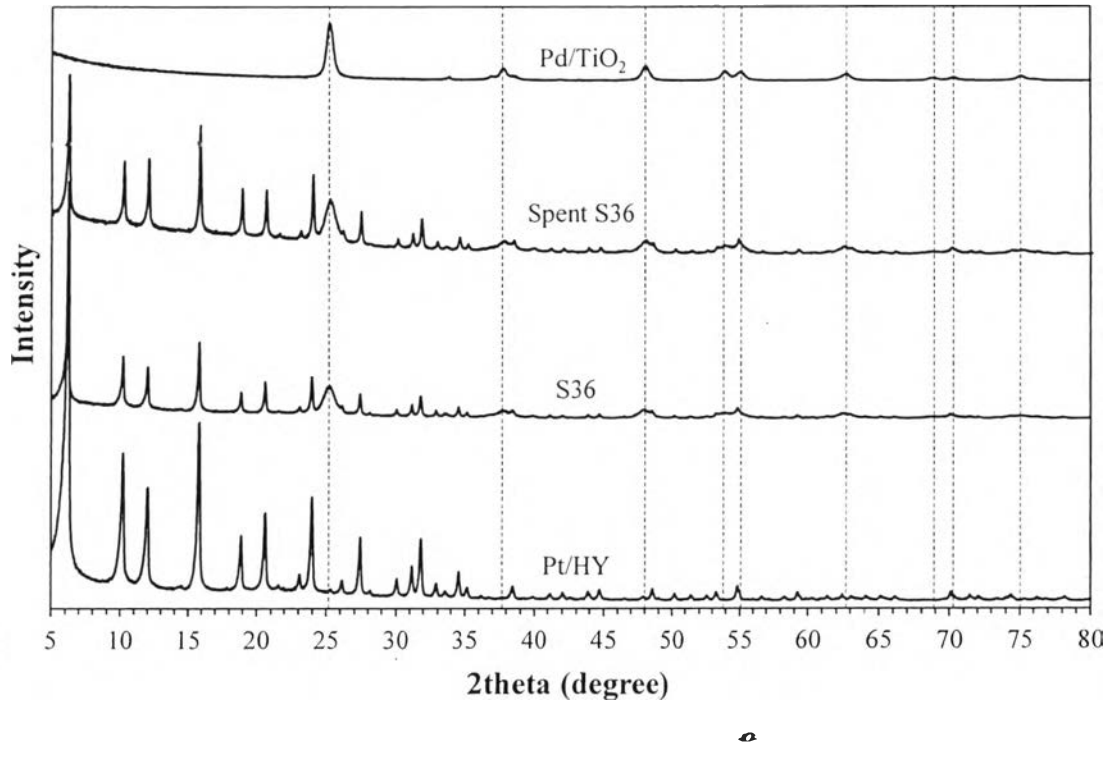

Figure 4.22 XRD patterns of Pt/HY, S36, Spent S36 and Pd/TiO_2 catalysts, (dashed line: anatase).